Thermal Aspects Related to Power Assemblies

Adrian PLESCA, Alina SCINTEE
Universitatea Tehnica Gheorghe Asachi din Iasi, Romania
aplesca@ee.tuiasi.ro

***Abstract*—In many cases when a power assembly based on power semiconductors is used, catastrophic failure is the result of steep temperature gradient in the localized temperature distribution. Hence, an optimal heatsink design for certain industrial applications has become a real necessity. In this paper, the Pro/ENGINEER software with the thermal simulation integrated tool, Pro/MECHANICA, has been used for thermal study of a specific power semiconductor assembly. A series of steady-state and transient thermal simulations have been performed. The experimental tests have confirmed the simulation results. Therefore, the use of specific 3D modeling and simulation software allows to design special power semiconductor assemblies with a better thermal transfer between its heatsink and power electronic components at given operating conditions.**

***Index Terms*—Heating, Modeling, Power assembly, Simulation software, Temperature**

I. Introduction

Power electronics is essential for the development of extremely dynamic, low-voltage applications such as high performance microprocessor computer systems and it is increasingly important to the automotive industry. For instance, power electronics is an enabling technology for the development of cleaner and more efficient vehicles. As a result, reliability, durability and cost become very crucial issues.

The present trend in power electronics design is towards high power density with larger heat dissipations despite a more compact package. Consequently, a powerful and effective thermal design must be applied to help sustain the trend of increased miniaturization of power electronics devices. Nevertheless, power electronics miniaturization and packaging is a new technical specialization area of power electronics. It is a combination of many technical study areas. As thermal management is one of these areas, good thermal design is an extremely important component in the development of reliable power electronics products.

Since power input to the electronics is converted to heat in several different forms, thermal science is playing an increasingly important role in the advancement of electronics technology. Examples of the different forms of heat losses are switching losses in semiconductors, dielectric losses, magnetic losses and ohmic losses in conductors and resistors.

The numbers of articles published, [1]-[9], and research efforts regarding various aspects of heat transfer in power electronics systems over the past ten years have far exceeded that in previous decades.

Devices of this type are usually used on a large scale where the heat flux levels are much greater than microelectronics.

In many cases, catastrophic failure is a result of steep temperature gradient in the localized temperature distribution. The local heat transfer characteristics are complex, as the heat dissipated in the chip is conducted into the substrate and then transferred by some combination of thermal conduction, convection and radiation to the outer surface through numerous components. This detailed distribution is commonly simplified by identifying a junction to case resistance; however, the variation over the complex surface could yield surface heat flux values ranging from 0.1 to 0.3 W/m^2 or more.

II. 3D Modeling and Simulation of a Power Semiconductor Assembly

Thermal analysis can be performed by a variety of methods. Simulation using numerical modeling is inherently a computationally intensive process, since there are many equations to be solved iteratively. Computer aided design (CAD) systems are used to describe geometrical models, to manipulate data and to display the results. Therefore, CAD systems with thermal analysis and computational fluid dynamics (CFD) modules become very powerful tools to investigate the thermal distribution within the electronics package, [10]-[16].

In this paper, a power assembly including MOS semiconductors and its heatsink has been studied from thermal point of view. This kind of power device in Figure 1 is used in automotive industry and it is the main component part in order to adjust the air conditioning speed inside the cars.

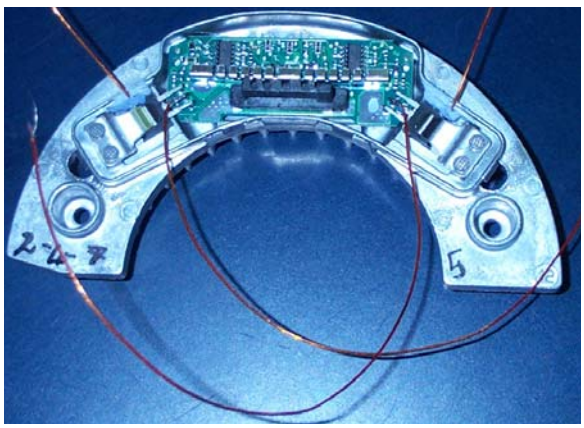

Figure 1. Power assembly sample.

A. Basic thermal theoretical aspects

The progress in computer technology enables the modeling of more and more complex structures in less time. It has therefore been the aim of this work to develop a 3D model of a complete power assembly based on power semiconductors type MOS.

Digital Object Identifier 10.4316/AECE.2010.01004

The starting point is the power balance equation for each volume element dV, in the integral formulation:

$$\iiint \frac{j^2}{\sigma} dV = \iiint \rho c \frac{\partial T}{\partial t} dV - \iiint div(\lambda \cdot gradT) dV \quad (1)$$

Where:
T means the temperature of element (ºC):
j – current density (A/m^2);
σ – electrical conductivity (1/Ωm);
ρ – material density (kg/m^3);
c – specific heat (J/kgºC);
λ – thermal conductivity (W/mºC).

The left term of the above equation denotes the heating power from the current flow. It is in balance with the heat stored by temporal change of temperature and the power removed from the element by thermal conduction. For the steady state temperature calculation, the heat storage term is zero and (1) becomes,

$$\iiint \frac{j^2}{\sigma} dV = -\iiint div(\lambda \cdot gradT) dV \quad (2)$$

The current density j, necessary in (1), follows from,

$$j_x = \sigma \frac{\partial U}{\partial x}, \quad j_y = \sigma \frac{\partial U}{\partial y}, \quad j_z = \sigma \frac{\partial U}{\partial z}, \quad j = \sqrt{j_x^2 + j_y^2 + j_z^2} \quad (3)$$

where U, is the electric potential that follows the Laplace equation:

$$div(\nabla U) = 0 \quad (4)$$

The current density j and the electric potential U must also satisfy the external circuit equation:

$$e(t) = L \frac{di}{dt} + Ri + U \quad (5)$$

where e(t), L and R are the external circuit characteristics.

B. Thermal model of the heatsink power assembly

Taking one's stand on the above thermal equations, first of all a 3D model for a typical heatsink power assembly has been developed using a specific software, the Pro-ENGINEER, an integrated thermal design tool for all type of accurate thermal analysis on devices. In order to reduce the simulation overhead, the mechanical drawing has been simplified by removing all the "unessential mechanical details" from thermal point of view in Fig. 2. The material used for the thermal model is cast aluminum with thermal conductivity about 130 W/m°C, thermal capacity of 963 J/kg°C and density about 2700 kg/m3.

C. Definition of the thermal exchange coefficient

One of the most important parameters involved into thermal modeling and simulation is the convection coefficient. This parameter has a great influence on the thermal exchange between heatsink and environment, determining, for the most part, the maximum temperature of the device.

From the experimental measurements, the value of thermal resistance heatsink-to-air, R_{thHA}, has been obtained.

This value is made of two main contributions:

- the conduction thermal resistance R_{thcond} which represents the heat conduction inside the heatsink from the thermal source to the boundary with the external environment;
- the convection thermal resistance R_{thconv} which represents the heat conduction from the heatsink boundary to the external environment.

Figure 2. Thermal model of the heatsink.

$$R_{thHA} = R_{thcond} + R_{thconv} \quad (6)$$

$$R_{thconv} = 1/(K_t A_H) \quad (7)$$

where K_t [W/°Cm^2] is the convection coefficient and A_H [m^2] is the heatsink area involved in thermal exchange.

The value of R_{thHA} has been obtained by means of an experimental test performed using a test bench. A power assembly sample has been equipped with two thermocouples mounted close to the MOSFETs case, Fig. 1. The sample has been heated using a test bench at a load current of 5 A. The forward drop voltage for the MOSFETs was about 4 V. The time evolution of the heatsink temperature has been recorded using the multi-channel scope. Therefore, the steady state heatsink temperature has been used to obtain the R_{thHA}, with the relation,

$$R_{thHA} = T_{HSS}/(V_{DS} \cdot I_{load}) \quad (8)$$

The heatsink temperature at the end of the test has been T_{HSS}=96.4°C.

Using the heatsink temperature values obtained from the above measurements, a series of thermal simulations has been performed in order to obtain the correct value for the convection coefficient. The best value for convection coefficient is 0.0197 mW/°Cmm^2, which corresponds to a temperature (at the same point where the thermocouple has been placed for the experimental test) of 96.47 °C, which is very close to the measured value, 96.4 °C. The thermal simulation with the final convection coefficient value is reported in Fig. 3.

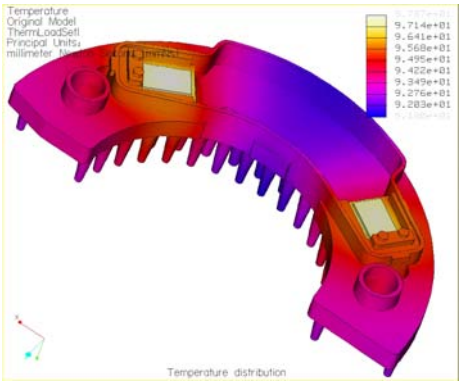

Figure 3. Thermal simulation of the heatsink with the optimum value of convection coefficient.

D. Thermal model of the MOS device

As in the previous case, in order to reduce the simulation overhead, the mechanical drawing of MOS has been simplified by removing all the "unessential mechanical details". The materials involved in the thermal model are presented in Table I.

TABLE I. MATERIAL THERMAL PROPERTIES

Material	Part thermal model	Thermal conductivity, λ (W/m°C)	Thermal capacity, c (J/kg°C)	Density, ρ (kg/m³)
Rhodorsil- Pâte	Compound	4.1	833	2200
Tamacc2 (copper)	Case	338	385	8960
Demelloy22	Solder	54	129	11170
Silicon	Die	124	702	2330
Aluminium	Wire bonds	200	900	2700

The dimensions of the copper leadframe have been obtained from drawings of a typical TO220 package and from measurements on a sample device. The die size is 4.45x5.65. As it can be noted the plastic moulding has been neglected since it should not contribute to the thermal exchange (it may have some effect during fast transients). The solder layer it has been assumed of uniform thickness. This is an arbitrary assumption which is the best we could do at present. A 0.1 mm thick compound layer has been applied at the bottom of the case. The thermal model has been used to perform a simulation in stationary conditions. The aim of this simulation has been to determine the thermal resistance junction to case (RTH_JC) of the device and compare it (for validation) with the data available on the datasheet. The total applied power is 50 W and the temperature of the bottom surface of the compound has been fixed to 40 °C. In Figure 4, the obtained temperature distribution is shown. The maximum junction temperature is TJMAX = 78 °C, while the temperature obtained for the measurement point placed on the device case at the interface with the compound layer is TCASE = 51 °C. From the above results, the value of RTHJC can be calculated as (TJMAX - TCASE)/50 = 0.53 °C/W. This compares well with the data reported on the datasheet which is 0.52 °C/W.

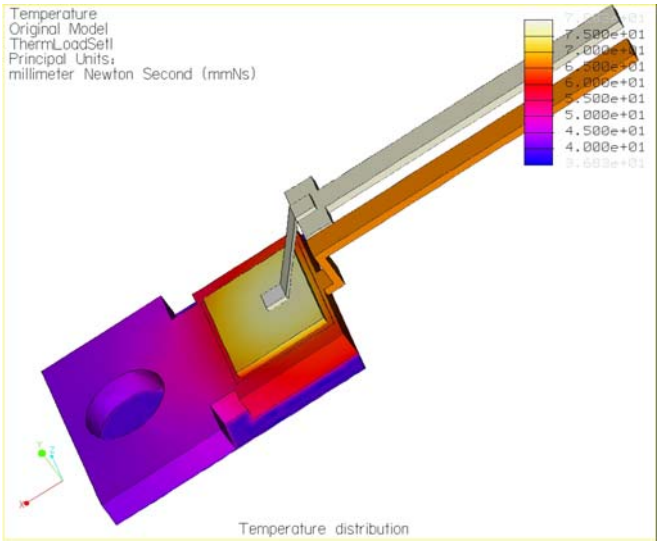

Figure 4. Thermal simulation in stationary conditions of the MOS device.

III. THERMAL MODELING OF POWER ASSEMBLY

The thermal simulations in this case have been set up with a total power of 20 W and the initial temperature of 40 °C. The power has been distributed on the die of both power semiconductor devices. The obtained thermal impedance curve is depicted in Figure 5. The curve refers to a measurement point on the heatsink placed below the centre of the MOS case.

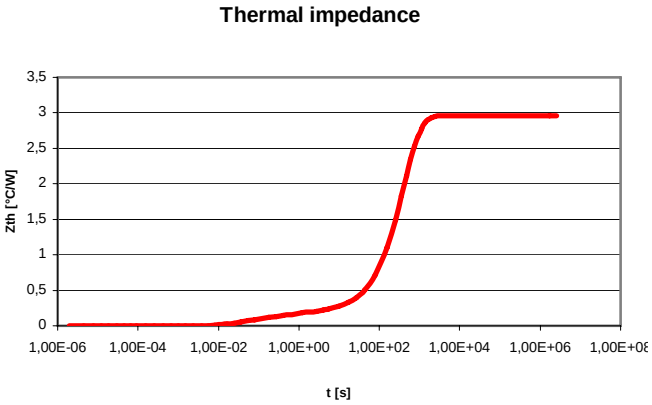

Figure 5. Thermal impedance curve of the heatsink.

From an analogous simulation, the thermal impedance curve of the MOS has been obtained. The curve is shown in Figure 6.

Both the heatsink and the device thermal impedance curves have been fitted with a series of exponential terms of the type of equation below,

$$Z_{th}(t) = R_{th\_1} \cdot \left(1 - e^{t/\tau_1}\right) + R_{th\_2} \cdot \left(1 - e^{t/\tau_2}\right) + \ldots + R_{th\_n} \cdot \left(1 - e^{t/\tau_N}\right) \quad (9)$$

In both cases, the number of exponential terms has been limited to three. In Table II, the obtained values for R_{thi} and τ_i are reported.

TABLE II. FITTED PARAMETERS

Component part	Exponential term n°	R_{th} [°C/W]	τ [s]
MOS device	1	0.206	0.00606
	2	0.0669	0.000215
	3	0.271	0.0874
Heatsink	1	0.480	245.15
	2	2.29	439.77
	3	0.187	0.172

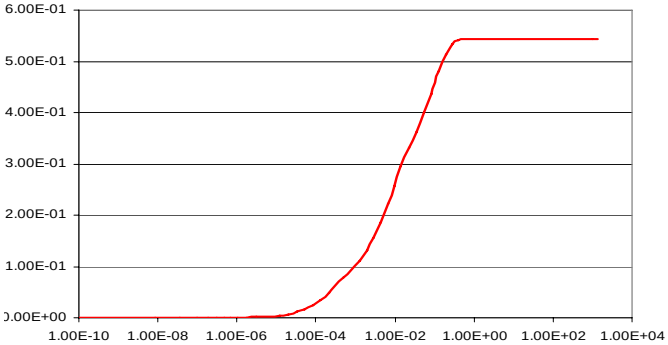

Figure 6. Thermal impedance curve of the MOS device.

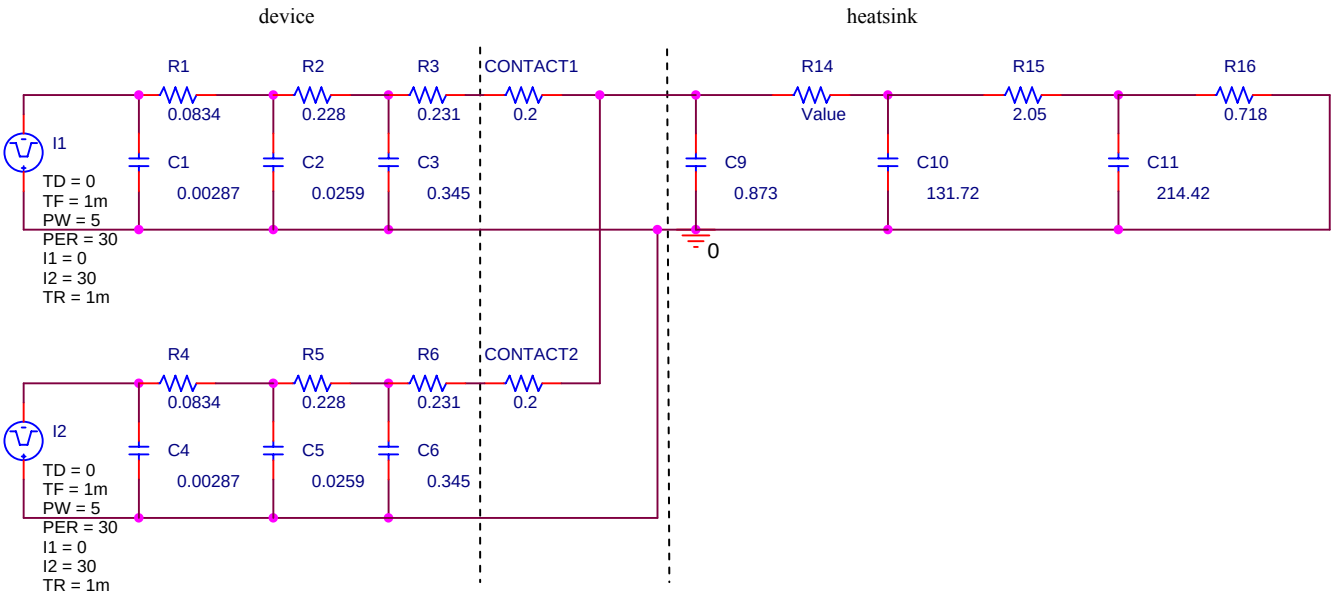

Figure 7. Thermal equivalent ladder network of the power assembly.

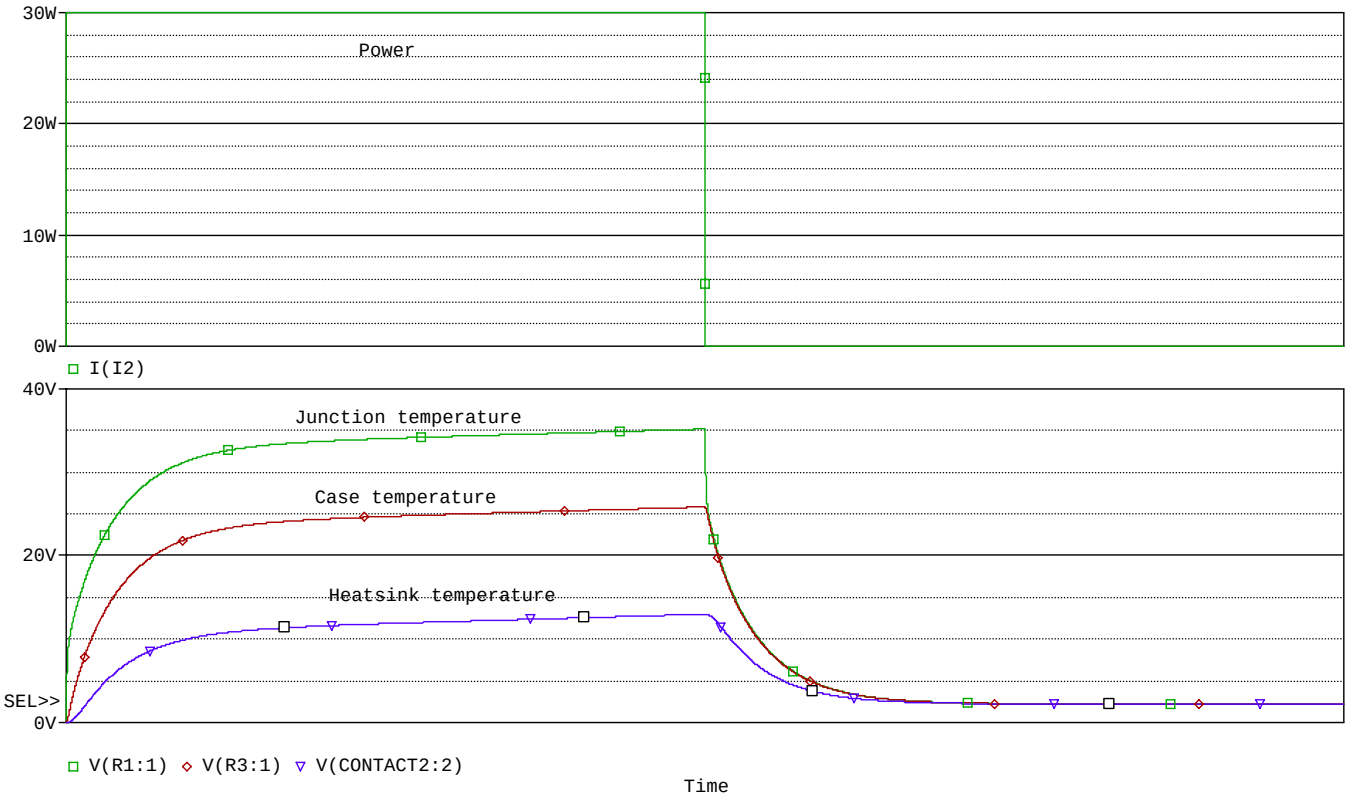

Figure 8. Test cycle simulation results of the power assembly.

The above parameters have been used for the synthesization of the equivalent ladder network. The synthesization method is based on the reduction of the rational function expressing the thermal impedance in the Laplace domain by means of successive polynomial divisions. The obtained values for R_i and C_i are reported in Table III. By using the above R and C values, the model can be reduced to the form depicted in Figure 7.

TABLE III. R AND C PARAMETERS

Component part	Cell n°	R	C
MOS device	1	0.0834	0.00287
	2	0.228	0.0259
	3	0.231	0.345
Heatsink	1	0.185	0.873
	2	2.05	131.72
	3	0.718	214.42

As it can be noted, a contact thermal resistance has been added between the device and the heatsink. The value assumed for this resistance is 0.2 °C/W. Using this simplified model, a simulation of the test cycle has been done. The results are reported in Figure 8. Because of the analogy between electrical and thermal quantities, the ordinate units actually mean temperature (not voltage because of the simulation software used).

As it can be noted, the heatsink temperature under the MOS case 0.1 s after the end of the cycle is about 12 °C, while the case temperature is 20 °C. These results are substantially confirming the measurements performed on the power assemblies samples.

IV. CONCLUSION

Further on, the main conclusions of the thermal study, with respect to the power assemblies based on power semiconductors, are presented.

- because of very complex thermal phenomenon, the thermal analysis can be done using a specific 3D FEM software (Pro-ENGINEER and Pro-MECHANICA); in this way, temperatures can be calculated anywhere inside of or on the power assembly;
- the steady-state thermal simulations allow to establish the convection coefficient;
- the transient thermal simulations allow to obtain the thermal impedance used for the synthesization of the equivalent ladder network based on thermal resistance and capacity;
- on the base of the equivalent ladder network, the simplified thermal model has been used for a test cycle;
- the use of the 3D simulation software can improve the power assembly design and, also, there is the possibility to get new solutions with an optimal thermal transfer.

REFERENCES

[1] C. J. M. Lasance (1995, October). "Electronics Cooling: The Need For A Change In Thermal Design Philosophy", Southborough, MA. [Online]. Available:http://www.electronicscooling.com/Resources/EC_Articles/OCT95/oct95_04.htm

[2] L. Mays and K. Kime, "Utilizing low forward voltage drop power semiconductors to minimize heat sinking requirements in multichip module DC solid state relays and static switching applications," in Proc. 1998 Multichip Modules and High Density Packaging Conf., pp. 149 – 154.

[3] Q. Qian, Y. Liu, Y. Liu, H. Yang, and S. Irving, "TO220 package lead frame optimization for reducing trim and form delamination by simulation", in Proc. 2005 Electronic Packaging Technology Conf., pp. 157 – 160.

[4] G. Rata, M. Rata, I. Graur, and L. D. Milici, "Induction Motor Speed Estimator Using Rotor Slot Harmonics", Advances in Electrical and Computer Engineering, vol. 9, Issue 1, pp. 70-73.

[5] S. Narasimhan and J. Majdalani, "Characterization of compact heat sink models in natural convection", IEEE Trans. Components and Packaging Technologies, vol. 25, Issue 1, pp. 78 – 86, March 2002.

[6] S. P. Watson and B. G. Sammakia, "The thermal performance of a chip scale package array with simple block and plate heat sinks", in Proc. 2002 Thermal and Thermomechanical Phenomena in Electronic Systems Conf., pp. 276 – 284.

[7] L. T. Yeh, "Effect due to a series of heat sinks on component temperatures", in Proc. 1998 Thermal and Thermomechanical Phenomena in Electronic Systems Conf., pp. 118 – 123.

[8] E. De Baetselier, W. Goedertier, and G. De Mey, "A survey of the thermal stability of an active heat sink", in Proc. 1996 Thermal Phenomena in Electronics Systems Conf., pp. 373 – 382.

[9] M. Rata, G. Rata, L. D. Milici, and I. Graur, "An Efficient Solution of the Step-down Converter for Students Teaching", Electronics and Electrical Engineering (Elektronika ir Elektrotechnika), no. 3(91), pp. 77-80, 2009.

[10] A. Shah, B. G. Sammakia, H. Srihari, and K. Ramakrishna, "A numerical study of the thermal performance of an impingement heat sink-fin shape optimization," IEEE Trans. Components and Packaging Technologies, vol. 27, Issue 4, pp. 710 – 717, Dec. 2004.

[11] S. Narasimhan, A. Bar-Cohen, and R. Nair, "Thermal compact modeling of parallel plate heat sinks," IEEE Trans. Components and Packaging Technologies, vol. 26, Issue 1, pp. 136 – 146, March 2003.

[12] J. R. Culham, M. M. Yovanovich, and S. Lee, "Thermal modeling of isothermal cuboids and rectangular heat sinks cooled by natural convection", IEEE Trans. Components, Packaging, and Manufacturing Technology, vol. 18, Issue 3, pp. 559 – 566, Sept. 1995.

[13] M. Rata, G. Rata, C. E. Bobric, "Three-phase PVM invertor with HEF4752", Advances in Electrical and Computer Engineering, vol. 3, Issue 1, pp. 90-93.

[14] T. S. Fisher, K. E. Torrance, and K. K. Sikka, "Analysis and optimization of a natural draft heat sink system" in Proc. 1996 Thermal Phenomena in Electronics Systems Conf., pp. 115 – 123.

[15] A. T. Morrison, "Optimization of heat sink fin geometries for heat sinks in natural convection," in Proc. 1992 Thermal Phenomena in Electronics Systems Conf., pp. 145 – 148.

[16] J. R. Culham and Y. S. Muzychka, "Optimization of plate fin heat sinks using entropy generation minimization", IEEE Trans. Components and Packaging Technologies, vol. 24, Issue 2, pp. 159 – 165, June 2001.

ACKNOWLEDGMENTS

This work was supported by PN II National Programme of Research, Development and Innovation - Ideas - Exploratory Research Projects, Project Code 352, Contract no.706/19.01.2009.